Received: 24 October 2022 | Revised: 21 February 2023 | Accepted: 21 February 2023

DOI: 10.1111/gcb.16667

Global Change Biology WILEY

RESEARCH ARTICLE

Satellite-based evidence highlights a considerable increase of urban tree cooling benefits from 2000 to 2015

Jiacheng Zhao[1,2,3] | Xiang Zhao[1,2] | Donghai Wu[4,5] | Naika Meili[3] | Simone Fatichi[3]

[1]State Key Laboratory of Remote Sensing Science, Faculty of Geographical Science, Beijing Normal University, Beijing, China

[2]Beijing Engineering Research Center for Global Land Remote Sensing Products, Faculty of Geographical Science, Beijing Normal University, Beijing, China

[3]Department of Civil and Environmental Engineering, National University of Singapore, Singapore, Singapore

[4]Key Laboratory of Vegetation Restoration and Management of Degraded Ecosystems, South China Botanical Garden, Chinese Academy of Sciences, Guangzhou, China

[5]Department of Ecology and Evolutionary Biology, Cornell University, Ithaca, New York, USA

Correspondence

Xiang Zhao, State Key Laboratory of Remote Sensing Science, Faculty of Geographical Science, Beijing Normal University, Beijing 100875, China.
Email: zhaoxiang@bnu.edu.cn

Donghai Wu, Key Laboratory of Vegetation Restoration and Management of Degraded Ecosystems, South China Botanical Garden, Chinese Academy of Sciences, Guangzhou 510650, China.
Email: donghaiwu@scbg.ac.cn

Funding information

National Natural Science Foundation of China, Grant/Award Number: 42090012; National University of Singapore, Grant/Award Number: 22-3637-A0001

Abstract

Tree planting is a prevalent strategy to mitigate urban heat. Tree cooling efficiency (TCE), defined as the temperature reduction for a 1% tree cover increase, plays an important role in urban climate as it regulates the capacity of trees to alter the surface energy and water budget. However, the spatial variation and more importantly, temporal heterogeneity of TCE in global cities are not fully explored. Here, we used Landsat-based tree cover and land surface temperature (LST) to compare TCEs at a reference air temperature and tree cover level across 806 global cities and to explore their potential drivers with a boosted regression tree (BRT) machine learning model. From the results, we found that TCE is spatially regulated by not only leaf area index (LAI) but climate variables and anthropogenic factors especially city albedo, without a specific variable dominating the others. However, such spatial difference is attenuated by the decrease of TCE with tree cover, most pronounced in midlatitude cities. During the period 2000–2015, more than 90% of analyzed cities showed an increasing trend in TCE, which is likely explained by a combined result of the increase in LAI, intensified solar radiation due to decreased aerosol content, increase in urban vapor pressure deficit (VPD) and decrease of city albedo. Concurrently, significant urban afforestation occurred across many cities showing a global city-scale mean tree cover increase of 5.3 ± 3.8% from 2000 to 2015. Over the growing season, such increases combined with an increasing TCE were estimated to on average yield a midday surface cooling of 1.5 ± 1.3°C in tree-covered urban areas. These results are offering new insights into the use of urban afforestation as an adaptation to global warming and urban planners may leverage them to provide more cooling benefits if trees are primarily planted for this purpose.

KEYWORDS

climate change, remote sensing, tree cooling efficiency, tree cover, urban afforestation

1 | INTRODUCTION

The drastic urban expansion to meet the requirements of a worldwide growing urban population has caused serious environmental problems (Foley et al., 2005; Grimm et al., 2008). Warmer temperature caused by urban heat islands (UHIs) exerts heat stress on urban ecosystems and can interact with heatwaves to exacerbate morbidity/mortality risk (Anderson & Bell, 2011; Patz et al., 2005; Zhao et al., 2018), which has been projected to worsen in the coming decades (Mora et al., 2017; Perkins-Kirkpatrick & Lewis, 2020).

Therefore, mitigation of urban heat has become an important target in current and future urban planning practices.

Afforestation is considered one prevalent solution among several biophysical solutions (e.g., reflective surfaces, modification of building materials, etc.) to reduce urban heat (McPherson et al., 2011). In past decades, tree-planting campaigns such as the million tree planting (McPherson et al., 2011; Moskell & Allred, 2013) and large-scale urban afforestation programs (Yao et al., 2019) have been launched globally to improve cities' overall sustainability (Nilon et al., 2017). As evidenced by remotely sensed observations, many cities are indeed experiencing the phenomenon of "green recovery" (Liu et al., 2020). However, the cooling benefits from such recent urban afforestation have not been evaluated on a global scale. Generally, urban areas fully covered by trees have much lower surface temperatures than treeless urban green spaces (Paschalis et al., 2021; Schwaab et al., 2021), which highlights the direct role of tree canopy cover (tree cover) in urban cooling. Tree canopy forms shade which reduces the amount of solar radiation that would otherwise heat the surface and provides also transpiration that shifts the partition of available energy from sensible to latent heating (Meili et al., 2021; Oke & Cleugh, 1987). However, trees' cooling effects vary substantially across cities. For example, planting trees in Los Angeles led to 5°C surface cooling for urban blocks with more than 30% tree cover when compared with blocks with less than 1% trees (Pincetl et al., 2012), while such difference was shown to be less than 3°C in Southeast Asian cities (Estoque et al., 2017).

The effectiveness of an increase in tree cover to cool urban areas can be measured by the tree cooling efficiency (TCE), which is defined as the temperature reduction for a 1% tree cover increase (Wang et al., 2019, 2020). TCE is regulated both by biophysical factors, for example, leaf area index (LAI), background climate, and human management (Rahman, Stratopoulos, et al., 2020; Speak et al., 2020). For instance, soil water availability is known to have a critical role in regulating trees' water use and transpiration rate at the seasonal or yearly scale (Luis et al., 2005; Zeppel et al., 2008). While at the daily scale air temperature (T_a) and humidity largely impact trees' transpirative flux, if trees are not under water stress, by modifying the vapor pressure deficit (VPD_L) between the leaf and the air (Chen et al., 2011; Gunawardena et al., 2017; Jim & Peng, 2012). Hot and dry conditions can lead to a considerably higher TCE as shown by both in situ measurements and remote sensing observations (Hamada & Ohta, 2010; Wang et al., 2019). Despite many of these factors having been suggested to have a close relationship to TCE, their combined effect on TCE and disentangled contribution to TCE across global cities are still unclear.

The use of an invariant TCE (Estoque et al., 2017; Wang et al., 2019, 2020; Zhou et al., 2017), usually expressed as the slope of a linear relationship between land surface temperature (LST) and tree cover, has recently been challenged. Compared with treeless urban areas, previous studies indicate those with high tree cover could locally have lower T_a but higher humidity due to substantial canopy transpiration, which results in a decreased local VPD_L that suppresses TCE (Wang et al., 2022; Yu et al., 2018). Hence, it is preferable to derive TCE for different tree cover levels and TCEs across cities are only comparable at similar tree cover levels (see Data S1 for a more detailed discussion). However, other mechanisms can modify how TCE is affected by tree cover because, for example, adding trees also changes urban canyon geometry and modify surface roughness, resulting in different efficiency of energy exchange. Studies have generally reported TCE to be greater in urban areas with low tree cover (Wang et al., 2022; Zhou et al., 2021), and it is worth exploring to what extent TCE can be suppressed by tree cover in different cities across the globe.

In the long term, TCE could change because of the variability in all the factors described above with a changing climate and urban growth. A changing TCE plays an important part in urban climate because it modifies canyon energy and water budgets, especially when accompanied with the large urban afforestation that is ongoing in many cities. The recent earth greening trend was suggested to enhance natural vegetation cooling effects in most regions (Chen et al., 2020; Forzieri et al., 2020), but how the cooling effects of urban trees responded to such a greening trend, especially in combination with a changing TCE, has not yet been quantified. Long-term exposure to a rising VPD may increase TCE through increasing transpiration or decrease TCE by reducing leaf stomatal conductance (Grossiord et al., 2020). In urban settings, VPD trends could be amplified along with accelerated urban expansion (Li et al., 2021; Meili et al., 2022). However, current information on TCE is mainly drawn from short-term observations or simulations over a few days (Ouyang et al., 2020) to months (Chen et al., 2019; Wang et al., 2020) and our understanding of the long-term dynamics of TCE as well as their causality with climate change remain limited.

2 | MATERIALS AND METHODS

2.1 | Tree cover data

We used the Landsat Vegetation Continuous Fields (VCF) tree cover layers (Sexton et al., 2013) that contain the percentage (%) of woody vegetation taller than 5 m in height in each 30-m pixel. The dataset is currently the only high-resolution tree cover for urban areas available at the global scale and was developed by downscaling the 250-m MODIS Vegetation Continuous Fields (VCF) products using all bands of the Landsat 5 Thematic Mapper (TM) and Landsat 7 Enhanced Thematic Mapper Plus (ETM+). Benchmarked with the MODIS VCF products, the Landsat dataset shows an RMSE of ~10% (Sexton et al., 2013) but depicts much more details on the fragmented patterns of urban trees (see an example of the data in Chicago, USA, Figure S1), thus providing us with sufficient tree cover details to establish its relationship with LST. The dataset is processed at an annual scale and for 2000, 2005, 2010, and 2015 (referred to as the 4 years thereafter), all of which were used for analyzing the spatial and temporal patterns of TCE. Tree cover derived from 30-m Landsat sensors can be underestimated to varying degrees as indicated by previous studies (Nowak & Greenfield, 2010; Pourpeikari

Heris et al., 2022) investigating the accuracy of the National Land Cover Dataset (NLCD). However, the global Landsat VCF tree cover layers used in this study reduce this underestimation as shown in two US cities: San Francisco and Washington selected as examples (Figure S2a,b).

2.2 | Land surface temperature data

We used the 30-m Landsat Level 2 LST provided by the United States Geological Survey (USGS) (Malakar et al., 2018). The data is derived from the Landsat Level 1 thermal infrared bands that are atmospherically corrected using a radiative transfer model and reanalysis data. It records the transient (~10:30 a.m. local time) radiative skin temperature of the land. The surface emissivity used for LST retrieval is first spectrally adjusted from the Advanced Spaceborne Thermal Emission and Reflection Radiometer (ASTER) global emissivity (Hulley et al., 2015) and then modified to account for vegetation phenology and snow cover using the Landsat surface reflectance data. By comparing ground-based measurements from six surface radiation budget (SURFRAD) network stations in the United States, the LST for Landsat 5 and Landsat 7 both show a mean bias of less than 1 K (absolute value) (Malakar et al., 2018). Given such good accuracy, the dataset has been often applied to analyze urban thermal conditions (Lu et al., 2020; Miller et al., 2022; Xian et al., 2022). For each LST image, we masked out pixels with cirrus, cloud, cloud shadow, high-level aerosol and water body based on the quality assessment (QA) bands generated by the CFMask algorithm (Foga et al., 2017). An example of the LST data in Chicago, USA, is shown in Figure S1.

2.3 | Reanalysis data

We used the ERA5-Land Climate Reanalysis product (Muñoz-Sabater et al., 2021), which is based on the land component of ERA5 to provide an accurate description of the past climate at an enhanced spatial resolution of 9 km (compared with 31 km in ERA5). It combines model data with observations from across the world into a globally complete and consistent dataset covering the temporal period from January 1950 to nearly the present. For each city, climate variables (e.g., T_a, precipitation, solar radiation, wind speed) were averaged over the growing season using the ERA5-Land Monthly data from the whole grids that cover the city area. The growing season is determined from the date when vegetation starts greening up to the date of dormancy indicated by the MODIS Global Vegetation Phenology product (MCD12Q2). The ERA5-Land Hourly data was also used to collect the T_a closest to each LST imaging time. VPD (kPa) in this study is calculated as

$$e_s = 0.611\exp\left(\frac{17.27T_a}{T_a + 237.3}\right) \quad (1)$$

$$e_a = 0.611\exp\left(\frac{17.27T_{dew}}{T_{dew} + 237.3}\right) \quad (2)$$

$$\mathrm{VPD} = e_s - e_a \quad (3)$$

where T_{dew} is dewpoint temperature (°C), e_s is saturation water vapor (kPa), and e_a is actual water vapor (kPa). We also used the Multi-Source Weather (MSWX) historical records (MSWX-Past) (Beck et al., 2022) as a supplementary to ERA5-Land. The meteorological product is based on ERA5 but bias-corrected using high-resolution reference climatology. It has a spatial resolution of 0.1° with global coverage from 1979 to nearly the present. Since MSWX includes relative humidity (%) rather than T_{dew}, the calculation of e_s using MSWX is the same as ERA5-Land but e_a is calculated as

$$e_a = \mathrm{RH} / 100 \times e_s \quad (4)$$

2.4 | Tree cooling efficiency and cooling benefits

TCE is defined as the temperature reduction for a 1% tree cover increase and can be expressed as the slope of a linear temperature–tree cover relationship (Wang et al., 2019). Although T_a is more relevant to thermal comfort than LST, in the long term, they tend to be connected (Manoli et al., 2020). Compared with T_a, LST directly affects the urban canopy energy budget, which in turn influences T_a. Satellite-based LST has been widely used to derive TCE (Wang et al., 2019, 2020, 2022; Yang et al., 2022; Zhou et al., 2021) because of its wide coverage, availability of long time series, spatial resolution, and acceptable accuracy. More discussion of using LST to derive TCE can be found in Data S1.

An invariant TCE from a linear LST–tree cover relationship would largely ignore the saturation of tree cooling effects at high tree cover levels. Thus, TCE in this study was generated from the slope (TCE = −ΔLST/Δtree cover) of a nonlinear relationship between LST and tree cover at different tree cover levels (Figure S3). For each city, the relationship was established with the following two steps. First, for each of the 4 years (i.e., 2000, 2005, 2010, and 2015), we collected all LST images covering the city in the growing season from Landsat 5, Landsat 7, and Landsat 8. Second, since the LST and tree cover images have a consistent spatial resolution of 30 m, each LST image was overlapped with the annual tree cover image and a nonlinear curve in form of $y = ax^b$ was fitted to the LST–tree cover scatters generated from all 30-m grids within the city boundary. Since the study focuses on the averaged TCE at the city scale, factors such as the difference in street canyon geometry, tree species and anthropogenic heat emissions affecting TCE at the neighborhood scale should be smoothed. Thus, we averaged the LST in each 1% tree cover bin and then fitted the binned scatters (Huang et al., 2015). Based on the curve, we calculated TCE at each tree cover level as a negative slope ($-abx^{b-1}$) where x denotes different tree cover levels (e.g., 10%, 20% and 30%). Figure S4 shows the city-scale LST–tree cover relationship in 16 cities across different climates, selected as examples.

For each city, each TCE derived from the established LST–tree cover relationships (one relationship for each LST image) describes the averaged urban tree midday (~10:30 a.m. local time) cooling potential. TCE changes with T_a because high T_a increases well-watered plant transpiration by enlarging VPD_L, leading to higher TCEs observed on hot summer days (Hamada & Ohta, 2010; Wang et al., 2019). To address this dependency, we collected the T_a closest to each LST image acquisition time based on ERA5-Land Hourly data and established linear TCE-T_a relationships for each tree cover level. Then, we compared TCE in global cities at a reference tree cover and T_a level (e.g., TCE.10.25 is the TCE at 10% tree cover, computed at 25°C T_a). Figure S5 shows the midday TCE–T_a relationship in 16 cities across different climates. Figure S6 shows how TCE changes with tree cover and T_a in New York and Rome, selected as examples.

We chose the reference T_a at 25°C for the TCE comparison because it is a temperature that is experienced by almost all global cities (close to the highest T_a in high-latitude cities and lowest T_a in tropical cities). However, we also compared the results from T_a at 20°C (i.e., TCE.10.20) and 30°C (i.e., TCE.10.30).

Based on the established TCE–tree cover relationships, we used a "space-for-time" substitution to estimate the city-scale cooling benefits from the mean increase of tree cover from x_1 to x_2 (Figure S3) as

$$\text{Cooling} = \int_{x_1}^{x_2} \text{TCE}\, dx \tag{5}$$

with

$$\text{TCE} = -\left(ax^b\right)' = -abx^{b-1} = -f_a f_b x^{f_b - 1} \tag{6}$$

where x denotes tree cover, f_a and f_b are the functions of T_a for parameters a and b in the TCE-tree cover relationship ($y = ax^b$), respectively. To simplify the calculation, we obtained constant f_a and f_b by linearly fitting midday-scale a and b versus T_a for each city. Then, the mean city-scale cooling benefits during the growing season were simply estimated using the growing season mean T_a ($\overline{T}_a$) as

$$\text{Cooling} = -\int_{x_1}^{x_2} f_a\left(\overline{T}_a\right) f_b\left(\overline{T}_a\right) x^{f_b\left(\overline{T}_a\right)-1} dx \tag{7}$$

Because TCE also changes with time, the mean cooling benefits in 2000 could be different from those in 2015 for the same increase in tree cover. Thus, the total cooling benefits for each city during the period 2000–2015 were obtained as the sum from six sub-periods (i.e., 2000–2002.5, 2002.5–2005, 2005–2007.5, 2007.5–2010, 2010–2012.5, and 2012.5–2015) considering tree cover changes in these sub-periods and the TCEs computed for the various periods were associated with their closest sub-periods (Equation 8). For example, the TCE in 2005 was used in the periods 2002.5–2005 and 2005–2007.5.

$$\text{Total cooling} = -\sum_{i=1}^{6} \int_{x_{1i}}^{x_{2i}} f_{ai}\left(\overline{T}_{ai}\right) f_{bi}\left(\overline{T}_{ai}\right) x^{f_{bi}\left(\overline{T}_{ai}\right)-1} dx \tag{8}$$

where i is the index expressing the sub-periods.

2.5 | Boosted regression tree and ecohydrological modeling

Boosted regression tree (BRT) is a tree-based machine learning model that addresses complex nonlinear relationships between dependent variables and predictors and uses the boosting technique to improve predictive performance (Elith et al., 2008). We used a BRT model to explain global spatial patterns of TCE and extract independent variables' partial effect and relative contribution. We used averaged TCE.10.25 from the 4 years as the dependent variable. Influential factors affecting TCE include biophysical traits, background climate, management level, and growing conditions (Rahman, Stratopoulos, et al., 2020). We accordingly selected several potential drivers as model inputs including LAI, the trend in LAI, cloud cover, solar radiation, wind speed, VPD, and city albedo. For LAI, we used the MODIS LAI 4-Day 500 m product (MCD15A3H). The trend in LAI from 2000 to 2015 was selected as a surrogate of vegetation management level. We used the MODIS Albedo Daily 500 m product (MCD43A3) (black-sky albedo for shortwave broadband was used) to represent the radiation-reflective properties of the city. Other climatic variables were all extracted from the two reanalysis datasets above. For each city, all these independent variables were averaged to a mean value during the growing season from the 4 years for model input. The number of trees in the BRT model was determined through a cross-validation (CV) procedure (Elith et al., 2008). Other parameters (e.g., learning rate, tree complexity) were optimized by improving the model's CV correlation with different combinations of the parameters (Table S1).

Although spatial drivers of TCE were explored by the BRT model, the effects of these drivers on the temporal change of TCE can hardly be explained by the BRT model. Hence, we further employed an urban ecohydrological model (Urban Tethys-Chloris, UT&C) (Meili et al., 2020) to disentangle mechanistically the independent contribution of LAI, climate variables and anthropogenic factors to the temporal change of TCE in two representative cities. This mechanism simulation is also used as a corroboration of the BRT model. Detailed UT&C model settings can be found in Data S1.

2.6 | Criterion of city selection and boundary

We first selected 1162 global cities, each with a total area greater than 50 km^2 based on the global urban boundaries (GUBs) dataset (Li et al., 2020) in 2000. Under the assumption that urban land is expanding, the use of the boundaries in 2000 ensures the analyses for the 4 years were all conducted in urban areas. Another advantage of fixing the boundary is that the change of tree cover would correspond with urban greening and not conflict with urbanization/expansion. With fixed city boundaries, tree planting or removal in the inner city is properly represented without confounding effects. Cities not covered by the tree cover data or the phenology data (MCD12Q2) were excluded from the analysis. Based on the NOAA Climate Data Record (CDR) of cloud products (Heidinger et al., 2014), we also excluded cities with an average cloud cover of more than 70% during the growing season. This is because a high level of cloud cover will result in too few LST pixels to obtain a reliable TCE and a large LST retrieval error would be expected for regions with high water vapor content (Jimenez-Munoz et al., 2014). Based on the Global Multi-resolution Terrain Elevation Data 2010 (GMTED2010) (Danielson & Gesch, 2011), we found that most cities in this study locate on flat land with a small variation of elevation (Figure S7) and we excluded a few cities with the standard deviation of elevation higher than 100 m. We further excluded cities with a very low correlation ($r^2 < 0.1$) between LST and tree cover. These filtering criteria finally resulted in the 806 selected cities.

3 | RESULTS

3.1 | Regional differences in tree cooling efficiency

Across global cities, TCE.10.25 (TCE at 10% tree cover, computed at 25°C T_a, see Section 2) showed substantial heterogeneity ranging from 0.01 to 0.47°C/% with a mean of 0.23 ± 0.08°C/% (Figure 1a,b). Strong TCE.10.25, larger than 0.31°C/%, occurred in cities on the west coast and northeast of North America, central-western Europe and Japan. In contrast, TCE.10.25 lower than 0.18°C/% are typically observed in cities in Central America, the Mediterranean coasts, Northern China and almost all cities in the southern hemisphere. However, this large spatial TCE discrepancy is diminished with increasing tree cover (Figure 1c–e) as a nonlinear LST–tree cover relationship leads to much lower TCE at higher tree cover. For instance, compared with the 10% tree cover at 25°C T_a, the mean difference of the TCE at 30% tree cover between European and South American cities reduced from 0.07 to 0.02°C/% (Figure 1c–e). During the growing season, TCE showed a high dependency on T_a (Figure S5; Figure 1f–h). For temperate and boreal cities, TCE.10.25 can be on average 35%–63% higher than TCE.10 at the mean T_a during the growing season (Figure 1f), implying urban trees' potential in providing more cooling benefits on hot summer days. While for tropical cities, this gap was reduced to at most 9% due to relatively stable T_a throughout the year.

Based on a BRT model, seven potential drivers explain almost 70% of the variance (training correlation = 0.845, cross-validation correlation = 0.678) of global TCE.10.25 (Figure 2). The drivers include one biophysical trait (LAI), four climatic variables (VPD, solar radiation, cloud cover and wind speed), and two anthropogenic factors (city albedo and the trend in LAI to represent tree management). Consistent with empirical data collected at the ground level (Rahman, Stratopoulos, et al., 2020), our model confirms that LAI at the global scale is still the most influential factor to improve TCE by increasing tree canopy total transpiration and providing more shading (Figure 2a,h). However, city albedo was also found to be an important factor in negatively affecting TCE (Figure 2b), which indicates, all else being equal, darker cities could have higher TCE than lighter ones. This is because trees replacing impervious darker surfaces with lower albedo reduce LST more than in cities with higher albedo. The modeling results using ERA5 and MSWX reanalysis products agree with each other on how climatic variables regulate TCE (Figure 2c–f). Spatially, plants growing in high VPD regions typically feature high transpirative demand but suffer from water stress, for example, the case of Mediterranean cities (Pares-Franzi et al., 2006; Rana et al., 2020). When irrigation is lacking, trees have to close their stomata and limit transpiration to preserve water and thus have low TCE (Zhao et al., 2023). The use of drought-tolerant species with low transpiration could be another explanation for the lower TCE in arid cities without irrigation. In contrast to VPD, solar radiation positively affects TCE (Figure 2d), which is likely because of the strong positive correlation between photosynthetically active radiation (PAR) and transpiration (Konarska et al., 2016; Wang et al., 2011). Meanwhile, decreasing cloud cover favors the increase in TCE (Figure 2e) because more cloud cover decreases the solar radiation received by the tree canopy. Generally, higher wind speed is expected to decrease tree canopy LST by reducing the aerodynamic and leaf boundary layer resistance and, thus, improving convection efficiency. However, this process may contribute even more efficiently to heat dissipation from impervious surfaces (e.g., roof), thereby reducing the LST difference between trees and impervious surfaces and thus decreasing TCE indirectly (Figure 2f). We used the trend in LAI here as a rough proxy of the vegetation management level. Developed cities are more likely to have advanced vegetation management that can reduce tree competition, provide better tree protection from pests and diseases and have more water accessibility (Konarska et al., 2016), all of which help improve urban trees' productivity and transpiration and thus TCE (Figure 2g).

3.2 | Temporal dynamics of tree cooling efficiency

We analyzed TCE's temporal dynamics by fitting the linear trend of TCE.10.25 from the 4 years 2000, 2005, 2010, and 2015. During the period 2000–2015, more than 90% of cities showed an increasing trend of TCE (Figure 3a) with a significant ($p < .05$, t-test) global mean TCE.10.25 increase of 45% from 0.2 to 0.29°C/%. Evident increases occurred mainly in northwest and eastern American and central-western European cities at a rate of more than 0.079°C/%/decade. We found these changes in TCE are mainly related to the recent vegetation greening and global climate change in different regions. In each of the six regions (Africa, Australia/New Zealand, Europe, North America, South America, and East Asia), we classified cities into a fast TCE increase group (TCE increasing rate larger than the regional median) and a slow TCE increase group (TCE increasing rate lower than the regional median). Despite large regional differences, almost all cities showed a positive greening rate indicated by the increasing trend in LAI (Figure 3b; Figure S8a) and all cities in fast TCE-increase groups showed higher greening rates than cities in slow TCE-increase groups.

Climatic variables also contributed to the temporal increase in TCE. In eastern American cities, for example, the

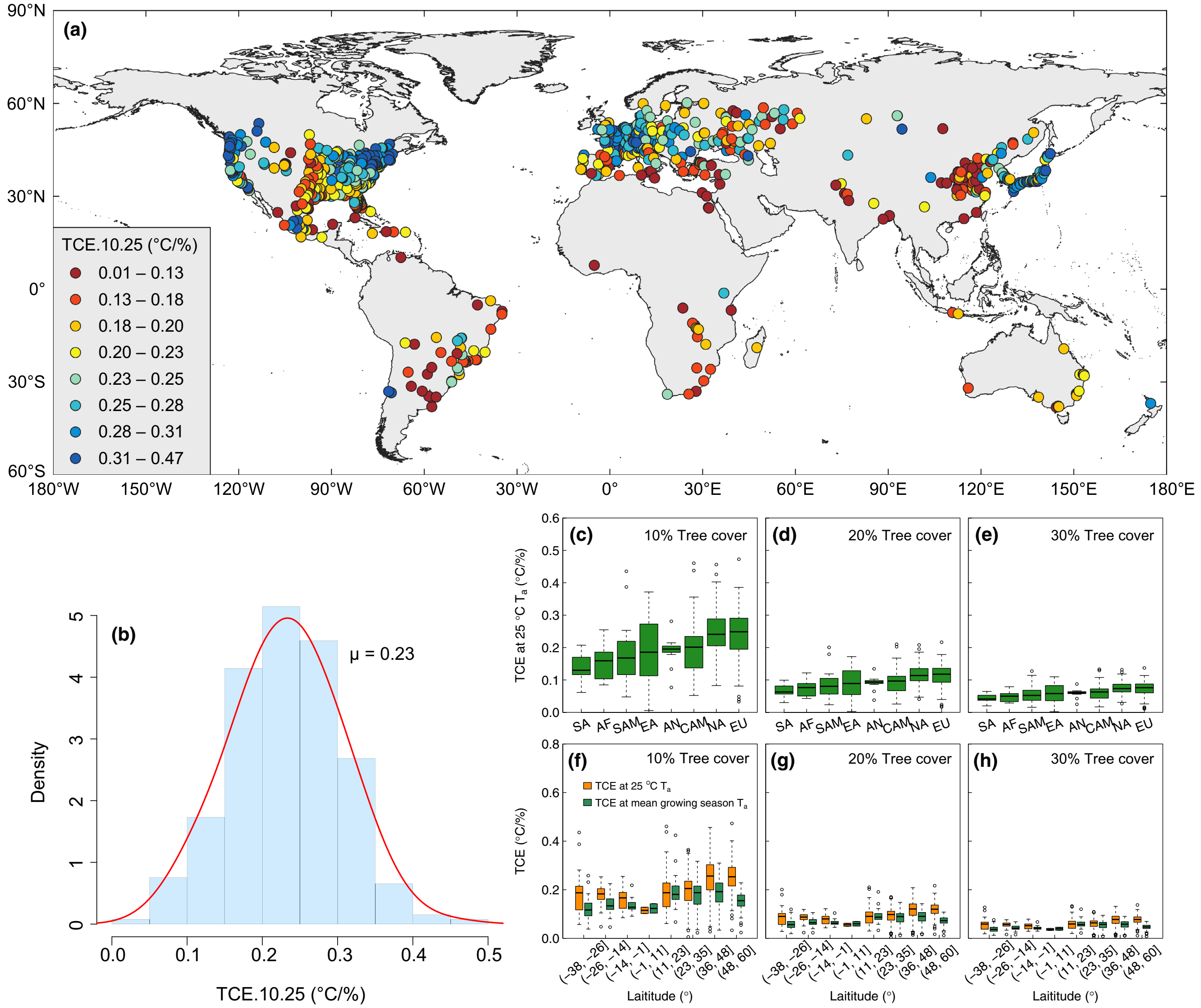

FIGURE 1 Tree cooling efficiencies (TCEs) of global large cities. Values are averaged from 4 years (i.e., 2000, 2005, 2010, and 2015). (a) TCE.10.25 of global large cities with urban areas greater than 50 km^2. Higher values suggest more surface cooling benefits from a 1% tree cover increase at 25°C T_a in an average 30 m × 30 m urban pixel with 10% tree cover. (b) Probability density distribution of TCE.10.25 with an expected value (μ = 0.23). (c–e) Regional comparison of TCEs at 25°C T_a for 10%, 20% and 30% tree cover, respectively. The regions include South Asia (SA), Africa (AF), South America (SAM), East Asia (EA), Australia/New Zealand (AN), Central America (CAM), North America (NA), and Europe (EU). (f–h) Comparison of TCEs at 25°C T_a and mean T_a during the growing season for 10%, 20%, and 30% tree cover across different latitudinal bands.

gradient change of increasing TCE trends from southeast to mid-west (Figure 3a) matches that of decreasing rates of aerosol optical depth (AOD) (Figure S8b). Decreasing AOD can improve TCE by increasing solar radiation (Figure 2d), leading to higher AOD decreases observed in fast TCE increase groups in most regions except for Europe (Figure 3c). However, records of surface solar radiation from SARAH-2 support the intensive increase of TCE in central Europe by showing a clear brightening (increasing solar radiation) trend over the analyzed period (Pfeifroth et al., 2018). Since TCE.10.25 is fixed at a reference T_a (25°C), the global warming-induced increase of saturation water vapor (e_s) is intrinsically removed. However, changes in relative humidity could still affect TCE by modifying the actual water vapor (e_a) of the air and thus VPD. Thus, intensive increases of TCE in the northwest and northeast American cities (Figure 3a) might be also related to their recent atmospheric drying trends with decreasing relative humidity (Figure S8c).

3.3 | Cooling benefits from tree cover increases

During the period 2000–2015, we found that not only TCE but also tree cover of more than 95% of the analyzed cities is

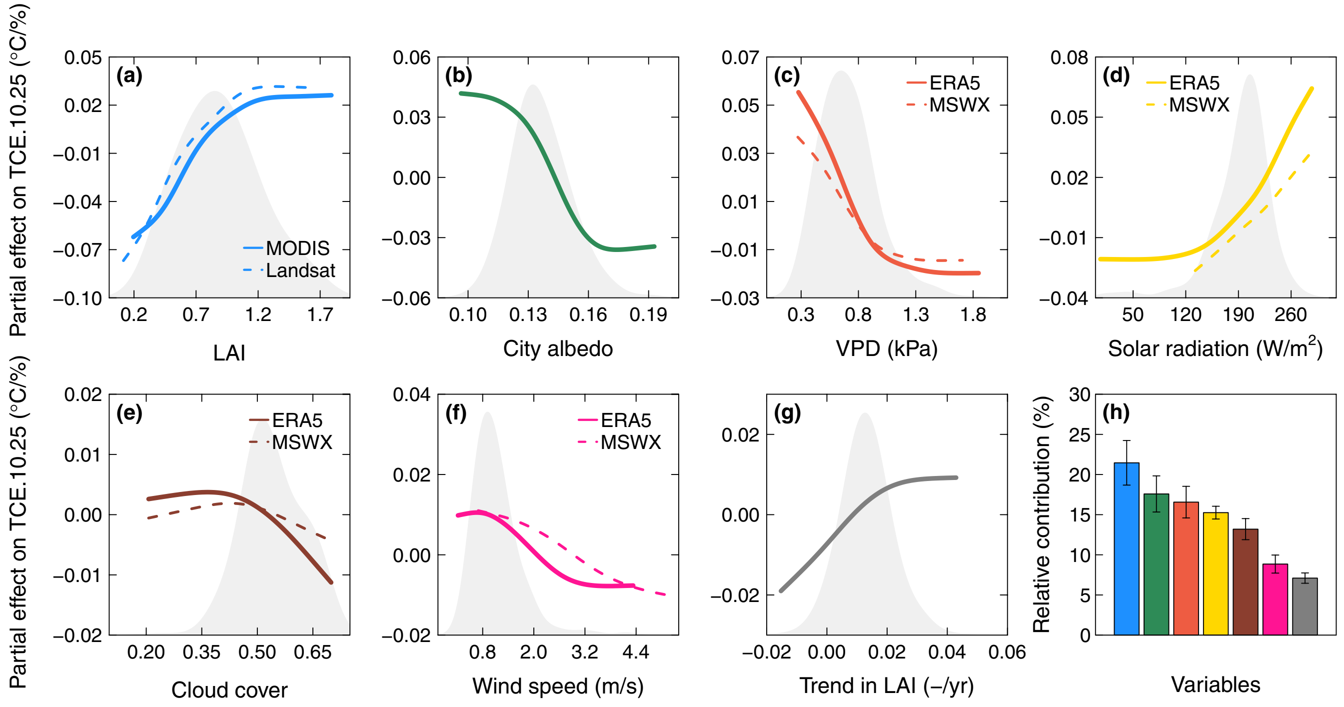

FIGURE 2 Determinants of global tree cooling efficiency (TCE). (a–g) Partial effects of different variables on TCE.10.25. TCE.10.25 values are averaged from 4 years (i.e., 2000, 2005, 2010, and 2015). The background shades are the probability density distributions of the variables. (h) Relative contribution (%) of each variable (blue for leaf area index [LAI], dark green for city albedo, orange for vapor pressure deficit, yellow for solar radiation, brown for cloud cover, pink for wind speed, and gray for the trend in LAI) to TCE.10.25. The error bars were derived from the variation of each variable contribution using different dataset combinations (MODIS LAI + ERA5, Landsat LAI + ERA5, MODIS LAI + MSWX, and Landsat LAI + MSWX).

increasing with a global mean increase of 5.3 ± 3.8% (Figure 4a). The most distinct tree cover increases (commonly more than 7%) were found in cities located in eastern North America and central-west Europe, followed by those near the west coast of the USA, in northern China, and quite a few South American cities. In contrast, cities located in west dry regions of the United States, southern Europe, and Africa showed minor tree cover increases (less than 3%). We used a "space-for-time" substitution (see Methods) to estimate how much cooling on average was yielded by the growing season tree cover increase combined with the increased TCE. We report a global mean surface cooling of 1.5 ± 1.2°C over tree-covered urban areas around midday (Figure 4b). Benefiting from both high tree cover increase, high TCE, and high TCE increasing rate, a strong cooling (>3°C, indicated by the arrows in Figure 4b) is clustered in the northeastern United States and central-west European cities. Cities with relatively low TCEs showed substantially lower surface cooling benefits as observed in the discrepancy between central-west Europe and northern Europe, where the tree cover increases are both high and comparable (Figure 4). The lowest cooling benefits (commonly less than 1.1°C) occurred in South American, South European, and African cities with both low tree cover increases, low TCEs, and slow TCE increasing rates.

4 | DISCUSSION

4.1 | Decreasing tree cooling efficiency with tree cover

Urban afforestation has vigorously increased in global cities since the late 20th century. Our satellite-based observations highlight a considerable increase of urban tree surface cooling benefits by considering a changing TCE and tree cover. For the first time, we compare 30-m TCE across cities at a given tree cover and T_a to provide a new global TCE pattern completely different from previous national/global analyses (Wang et al., 2020; Yang et al., 2022). Such a large difference comes from the fact that TCE changes with daily T_a and saturates at high tree cover (Figure S4), which is mechanistically supported by UT&C simulations (Figure S9a,b). More trees in a typical urban canyon can not only decrease local VPD_L but increase aerodynamic resistance (particularly in the example of Zurich, Figure S9c,d) by causing a smoother canyon fabric (Meili et al., 2021), both of which decrease the latent heat (or equivalently evapotranspiration, ET) efficiency (i.e., latent heat or ET change per tree cover change, Figure S9e,f) and thus TCE. Although TCE saturation has been reported in individual cities, as well from cross-city comparison, our global analyses extend the current understanding of the spatial

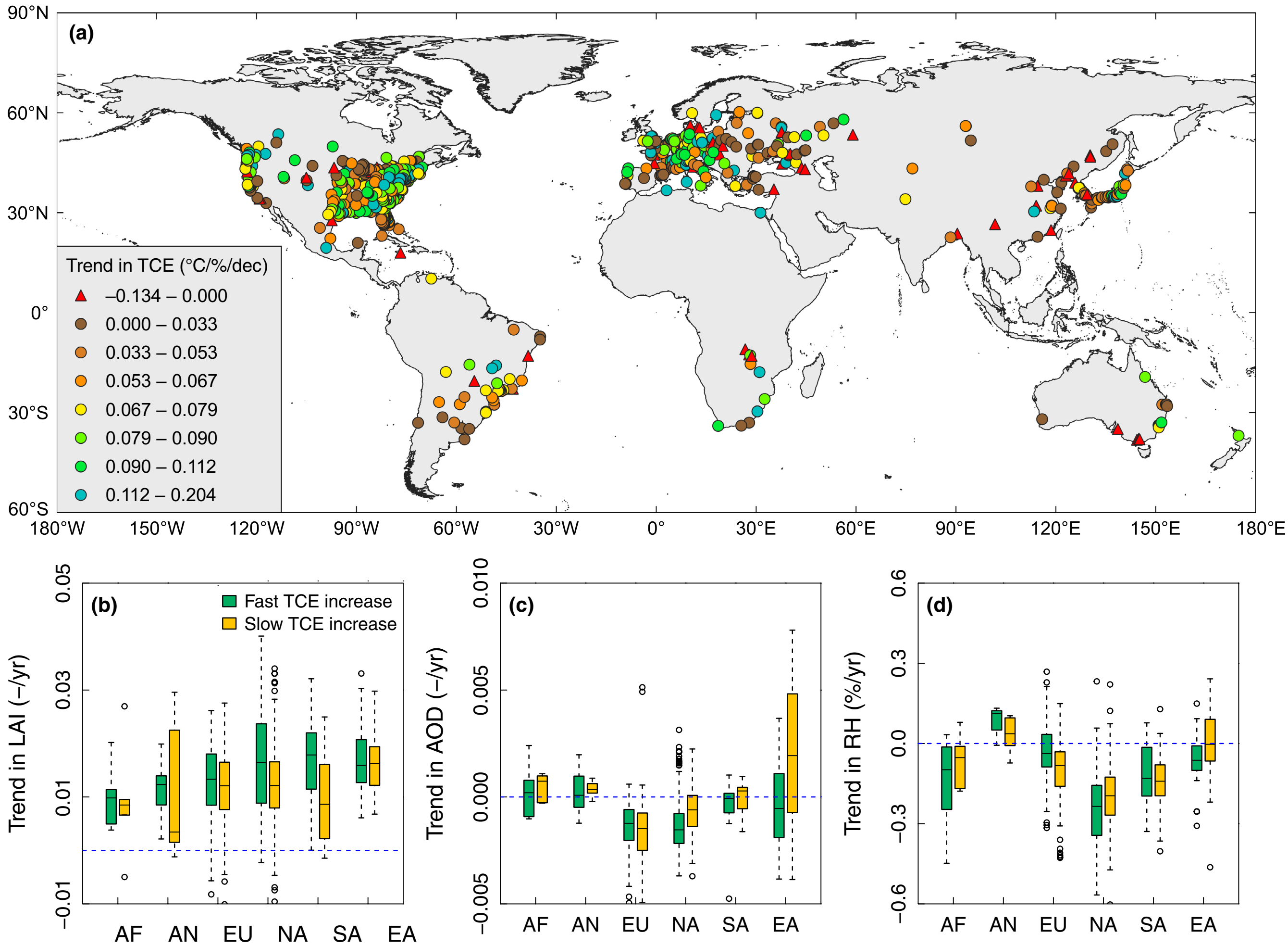

FIGURE 3 Temporal dynamics of tree cooling efficiency (TCE). (a) Global trends in TCE.10.25 (°C/%/decade) during the period 2000–2015. Points represent positive trends while red triangular symbols represent negative trends. (b-d) Comparisons of the trends in leaf area index (b), aerosol optical depth (c) and relative humidity (d) in different TCE groups (fast TCE-increase group vs. slow TCE-increase group) across six regions (AF = Africa, AN = Australia/New Zealand, EU = Europe, NA = North America, SA = South America, EA = East Asia). For each region, the cities with TCE increase rates larger than the regional median were grouped into the fast TCE increase group, while the cities with TCE increase rates lower than the regional median were grouped into the slow TCE increase group.

dependency of such saturation, as a much stronger TCE decrease with increasing tree cover is observed in midlatitude humid cities of the northern hemisphere (Figure 1).

4.2 | Factors regulating tree cooling efficiency and its role in cooling benefits

The global TCE pattern is a combined result of not only tree properties (e.g., LAI) but climate variables and anthropogenic factors especially city albedo, without a specific factor dominating the others even though LAI contributes the most. It should be noted that the use of TCE.10.25 helps disentangle VPD effects from T_a and reveals the bidirectional impacts of VPD, that is, spatially VPD has a detrimental effect on TCE.10.25 and any other characteristic value of TCEs (e.g., TCE.20.25) at a reference T_a, while temporally increasing VPD (e.g., decreasing relative humidity) can improve TCE, especially in locations where urban trees do not experience water stress.

Prominent surface cooling from large-scale urban afforestation observed in cities in the northeastern United States and central-west Europe (Figure 4) highlights the direct impacts of tree cover on surface heat mitigation despite that these regions also have the highest TCE.10.25 (Figure 1). However, TCE plays a greater role in urban areas with low tree cover, which results in comparable cooling benefits in northern Chinese cities from fewer increases of tree cover compared with central-west European cities (Figure 4).

4.3 | Increasing trend in tree cooling efficiency

The global increase of TCE since 2000 implies that for the same tree cover, urban trees now are providing more cooling benefits than they did two decades ago, especially in those European and eastern

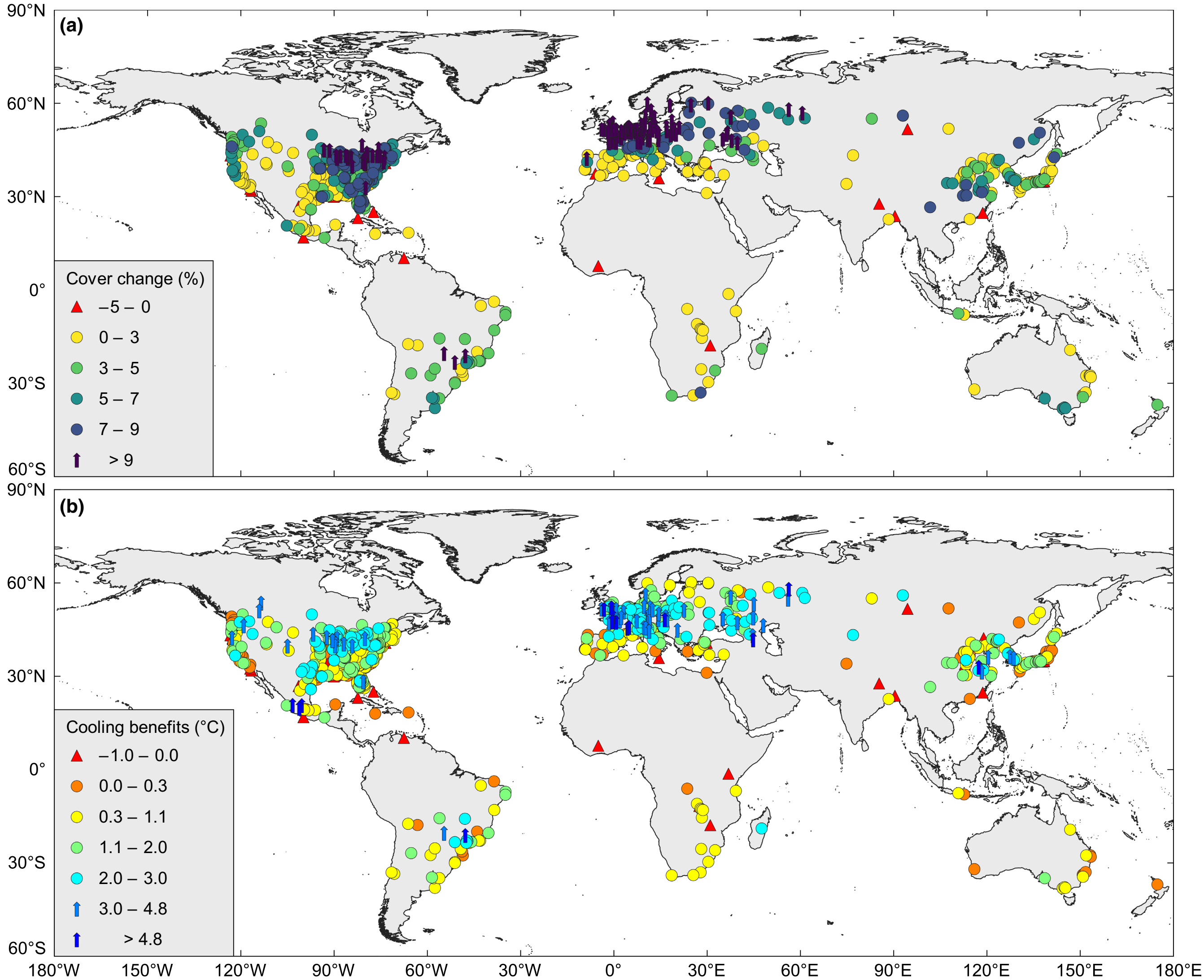

FIGURE 4 Cooling benefits from the increase of tree cover and tree cooling efficiency (TCE). (a) Changes in tree cover of global cities from 2000 to 2015. The value for each city is averaged over all 30 m × 30 m pixels within the city boundary. Circles and upward arrows represent increased tree cover (i.e., urban afforestation) during the analyzed period. Red triangular symbols represent decreased tree cover (i.e., urban deforestation). (b) Mean midday cooling benefits during the growing season from increased tree cover and TCE during the period 2000–2015. Red triangular symbols represent urban surface warming due to deforestation.

US cities with fast TCE increases. This is likely the result of the recent increase of LAI in Europe and decreased AOD in the United States. Other datasets also show a significant increase in LAI in the eastern United States (Zhu et al., 2016). However, increases of TCE could also be a result of changes in city albedo and atmospheric drying as relative humidity is decreasing in cities experiencing intensive urbanization as observed from global urban meteorological stations (Meili et al., 2022). From the perspective of the energy balance, the presented simulations also support this outcome by suggesting the individual contribution of a 1 unit LAI increase to latent heat increase and sensible heat decrease, at least in two midlatitude temperate cities, is comparable with the contribution of a 10% relative humidity decrease (Figure S10a–d). From the perspective of the tree-to-roof temperature difference (T_{tree}–T_{roof}), a decrease in albedo can cause much more increases of midday T_{tree}–T_{roof} (more than 1°C from 0.05 albedo decrease, Figure S10e,f) than other climate variables such as wind speed (less than 0.5°C from 20% wind speed decrease Figure S10g,h). The simulations indicate that the contributions of changes in relative humidity and albedo may be comparable with or potentially even larger than that of LAI especially as LAI increased from 2000 to 2015 by far less than 1 unit (at least as in the MCD15A3H dataset, Figure S8a). However, more observations and additional simulations are needed to support these conclusions.

It should be noted that in reality the increasing TCE could be even higher than our estimate because the use of TCE.10.25 ignores effects associated with global rising T_a. At least in the next decades, a continuation of such an increase could be expected due to continuing global warming and atmospheric drying (Cook et al., 2014; Ficklin & Novick, 2017), both of which can change more drastically in urban areas with a combination of UHIs and urban dry islands.

Our results are thus clearly confirming the benefits of enlarging city-scale afforestation to combat urban heat in the upcoming decades as promoted in many US and European cities (Young, 2011). For example, Baltimore plans to double its overall tree cover from 20% to 40% (Young, 2011) while London aims at a target of 50% by 2050 (Mayor of London, 2018). Nonetheless, tree planting should be strategically arranged especially in cities with strong TCE saturation because most surface-temperature benefits are likely realized in those neighborhoods or local areas with open trees and low tree covers.

4.4 | Challenges and necessity of dynamic monitoring

In the long term, a continuation of the enhanced urban tree ecosystem service (e.g., more cooling benefits from increasing TCE) could be challenging in a warming climate with rising VPD and soil drying. Long-term trends in VPD can enhance plant transpiration and soil water uptake, accelerating soil drying and contributing to plant water stress, which has been projected to be more frequent and severe in the coming decades (Brodribb et al., 2020; Grossiord et al., 2017, 2020). In the future, cities may need additional water for irrigation to fulfill the increasing water demand to ensure plant transpiration. More sophisticated urban greening management is required for both wet and dry cities given the potential for enhanced tree water stress and associated mortality (Allen et al., 2015; Carnicer et al., 2011; McDowell & Allen, 2015; Peng et al., 2011).

Given the importance (e.g., ecological, economic, landscape values) and distinctiveness (e.g., special growing conditions, vulnerability) of urban trees, their long-term monitoring in many cities is necessary but largely lacking. Prolonged monitoring of urban tree biophysical traits (e.g., LAI, transpiration, cooling potential and resilience) can provide us with robust information about how they acclimatize and respond to disturbances from climate change and urban development. So far, existing implications related to urban trees' cooling effects were mostly drawn from observations over short periods and single cities (Chen et al., 2019; Rahman, Hartmann, et al., 2020; Zheng et al., 2021), which may largely ignore temporal variability and bring biased assessments (Zhao et al., 2021). At the regional scale, our results suggest that the use of an invariant TCE from 2000 to estimate the total surface cooling benefits from urban afforestation during the period 2000–2015 could cause 0.3°C underestimation of these benefits, while the use of an invariant TCE from 2015 causes up to 1°C overestimation (Figure S11). At the city scale, much larger deviations could be expected in cities experiencing a rapidly changing climate and/or large tree cover change.

4.5 | Limitations

Our global results have limitations in terms of data and method applicability. Although the Landsat VCF used in this study improves the underestimation issues of tree cover (Figure S2), such underestimation may still exist in the Landsat-based tree cover dataset and could cause biased TCE. Our sensitivity tests show that the TCE derived from underestimated tree cover datasets could also be slightly underestimated (Figure S12). Despite the use of a 30-m spatial resolution, the TCE in this study was derived at the city scale and, therefore, it averages local heterogeneities. Combined with the change of tree cover aggregated from single pixels to the whole city, the inferred LST reduction then represents an averaged city-scale cooling benefit from the tree cover increase in a typical 30 m × 30 m urban pixel. However, actual local cooling could be dependent on tree species, tree arrangement (aggregated or sparse) (Myint et al., 2015; Zhao et al., 2020) and other elements such as impervious surfaces, grassland and water bodies that exist in the 30-m pixels and affect LST, which effects are simply averaged over the city. Although we used binned methods (see Section 2) to reduce the impacts of such fine-scale effects, they are unlikely to be fully eliminated (see Data S1 for a further discussion of the limits of TCE). The UT&C simulation indicates a lower TCE than that derived from the Landsat observations (Figure S9a,b). This is likely because UT&C simulates a change of tree cover in a prescribed low-rise urban canyon and the Landsat observations cover whole urban areas including urban forests that enlarge the temperature gradient from low to high tree cover.

5 | CONCLUSIONS

This study quantifies for the first time the global temporal–spatial patterns of the TCE at a reference tree cover and T_a in combination with the midday surface cooling benefits obtained from recent urban afforestation in large cities worldwide. During the period 2000–2015, the cooling achieved an average of 1.5°C, while it can be more than 3°C for specific cities with large tree planting campaigns, high TCEs and/or high TCE increasing rates. Urban planners may leverage these results to increase cooling benefits (Paschalis et al., 2021) if trees are primarily planted for this purpose. However, further tree expansion in already vegetated urbanscapes must be implemented with care given the saturation of TCE at large canopy cover and other costs of urban trees in terms of irrigation requirements and maintenance. With aggravating heat stress both from urbanization and global warming, proper urban afforestation is a low-carbon adaptation measure that has contributed to lower surface temperatures at an increasing rate over recent decades and it might still do so where tree cover is not very large and climate conditions are favorable.

ACKNOWLEDGMENTS

This work is supported by the National Natural Science Foundation of China (No. 42090012) and the National University of Singapore through the project "Bridging scales from below: The role of heterogeneities in the global water and carbon budgets," Award No. 22-3637-A0001. We thank the two anonymous reviewers for their constructive comments that improved the quality of the manuscript.

CONFLICT OF INTEREST STATEMENT

The authors declare that they have no conflict of interest.

DATA AVAILABILITY STATEMENT

The data and R code that support the findings of this study are available in a GitHub public repository (https://github.com/jiachengzhao/tree-cooling-efficiency).

ORCID

Jiacheng Zhao https://orcid.org/0000-0002-1493-4723
Xiang Zhao https://orcid.org/0000-0002-0155-6735
Donghai Wu https://orcid.org/0000-0002-4638-3743
Naika Meili https://orcid.org/0000-0001-6283-2134
Simone Fatichi https://orcid.org/0000-0003-1361-6659

REFERENCES

Allen, C. D., Breshears, D. D., & McDowell, N. G. (2015). On underestimation of global vulnerability to tree mortality and forest die-off from hotter drought in the Anthropocene. *Ecosphere*, *6*(8), art129. https://doi.org/10.1890/es15-00203.1

Anderson, G. B., & Bell, M. L. (2011). Heat waves in the United States: Mortality risk during heat waves and effect modification by heat wave characteristics in 43 U.S. communities. *Environmental Health Perspectives*, *119*(2), 210–218. https://doi.org/10.1289/ehp.1002313

Beck, H. E., van Dijk, A. I. J. M., Larraondo, P. R., McVicar, T. R., Pan, M., Dutra, E., & Miralles, D. G. (2022). MSWX: Global 3-hourly 0.1° bias-corrected meteorological data including near-real-time updates and forecast ensembles. *Bulletin of the American Meteorological Society*, *103*(3), E710–E732. https://doi.org/10.1175/bams-d-21-0145.1

Brodribb, T. J., Powers, J., Cochard, H., & Choat, B. (2020). Hanging by a thread? Forests and drought. *Science*, *368*(6488), 261–266. https://doi.org/10.1126/science.aat7631

Carnicer, J., Coll, M., Ninyerola, M., Pons, X., Sanchez, G., & Penuelas, J. (2011). Widespread crown condition decline, food web disruption, and amplified tree mortality with increased climate change-type drought. *Proceedings of the National Academy of Sciences of the United States of America*, *108*(4), 1474–1478. https://doi.org/10.1073/pnas.1010070108

Chen, C., Li, D., Li, Y., Piao, S., Wang, X., Huang, M., Gentine, P., Nemani, R. R., & Myneni, R. B. (2020). Biophysical impacts of earth greening largely controlled by aerodynamic resistance. *Science Advances*, *6*(47), eabb1981. https://doi.org/10.1126/sciadv.abb1981

Chen, L., Zhang, Z., Li, Z., Tang, J., Caldwell, P., & Zhang, W. (2011). Biophysical control of whole tree transpiration under an urban environment in northern China. *Journal of Hydrology*, *402*(3–4), 388–400. https://doi.org/10.1016/j.jhydrol.2011.03.034

Chen, X., Zhao, P., Hu, Y., Ouyang, L., Zhu, L., & Ni, G. (2019). Canopy transpiration and its cooling effect of three urban tree species in a subtropical city- Guangzhou, China. *Urban Forestry & Urban Greening*, *43*, 126368. https://doi.org/10.1016/j.ufug.2019.126368

Cook, B. I., Smerdon, J. E., Seager, R., & Coats, S. (2014). Global warming and 21st century drying. *Climate Dynamics*, *43*(9–10), 2607–2627. https://doi.org/10.1007/s00382-014-2075-y

Danielson, J. J., & Gesch, D. B. (2011). *Global multi-resolution terrain elevation data 2010 (GMTED2010)*. US Department of the Interior, US Geological Survey Washington, DC, USA.

Elith, J., Leathwick, J. R., & Hastie, T. (2008). A working guide to boosted regression trees. *The Journal of Animal Ecology*, *77*(4), 802–813. https://doi.org/10.1111/j.1365-2656.2008.01390.x

Estoque, R. C., Murayama, Y., & Myint, S. W. (2017). Effects of landscape composition and pattern on land surface temperature: An urban heat Island study in the megacities of Southeast Asia. *Science of the Total Environment*, *577*, 349–359. https://doi.org/10.1016/j.scitotenv.2016.10.195

Ficklin, D. L., & Novick, K. A. (2017). Historic and projected changes in vapor pressure deficit suggest a continental-scale drying of the United States atmosphere. *Journal of Geophysical Research: Atmospheres*, *122*(4), 2061–2079. https://doi.org/10.1002/2016jd025855

Foga, S., Scaramuzza, P. L., Guo, S., Zhu, Z., Dilley, R. D., Beckmann, T., Schmidt, G. L., Dwyer, J. L., Joseph Hughes, M., & Laue, B. (2017). Cloud detection algorithm comparison and validation for operational Landsat data products. *Remote Sensing of Environment*, *194*, 379–390. https://doi.org/10.1016/j.rse.2017.03.026

Foley, J. A., Defries, R., Asner, G. P., Barford, C., Bonan, G., Carpenter, S. R., Chapin, F. S., Coe, M. T., Daily, G. C., Gibbs, H. K., Helkowski, J. H., Holloway, T., Howard, E. A., Kucharik, C. J., Monfreda, C., Patz, J. A., Prentice, I. C., Ramankutty, N., & Snyder, P. K. (2005). Global consequences of land use. *Science*, *309*(5734), 570–574. https://doi.org/10.1126/science.1111772

Forzieri, G., Miralles, D. G., Ciais, P., Alkama, R., Ryu, Y., Duveiller, G., Zhang, K., Robertson, E., Kautz, M., Martens, B., Jiang, C., Arneth, A., Georgievski, G., Li, W., Ceccherini, G., Anthoni, P., Lawrence, P., Wiltshire, A., Pongratz, J., … Cescatti, A. (2020). Increased control of vegetation on global terrestrial energy fluxes. *Nature Climate Change*, *10*(4), 356–362. https://doi.org/10.1038/s41558-020-0717-0

Grimm, N. B., Faeth, S. H., Golubiewski, N. E., Redman, C. L., Wu, J., Bai, X., & Briggs, J. M. (2008). Global change and the ecology of cities. *Science*, *319*(5864), 756–760. https://doi.org/10.1126/science.1150195

Grossiord, C., Buckley, T. N., Cernusak, L. A., Novick, K. A., Poulter, B., Siegwolf, R. T. W., Sperry, J. S., & McDowell, N. G. (2020). Plant responses to rising vapor pressure deficit. *The New Phytologist*, *226*(6), 1550–1566. https://doi.org/10.1111/nph.16485

Grossiord, C., Sevanto, S., Borrego, I., Chan, A. M., Collins, A. D., Dickman, L. T., Hudson, P. J., McBranch, N., Michaletz, S. T., Pockman, W. T., Ryan, M., Vilagrosa, A., & McDowell, N. G. (2017). Tree water dynamics in a drying and warming world. *Plant, Cell & Environment*, *40*(9), 1861–1873. https://doi.org/10.1111/pce.12991

Gunawardena, K. R., Wells, M. J., & Kershaw, T. (2017). Utilising green and bluespace to mitigate urban heat island intensity. *Science of the Total Environment*, *584-585*, 1040–1055. https://doi.org/10.1016/j.scitotenv.2017.01.158

Hamada, S., & Ohta, T. (2010). Seasonal variations in the cooling effect of urban green areas on surrounding urban areas. *Urban Forestry & Urban Greening*, *9*(1), 15–24. https://doi.org/10.1016/j.ufug.2009.10.002

Heidinger, A., Foster, M., Walther, A., Zhao, X., & Program, N. (2014). *NOAA climate data record (CDR) of cloud properties from AVHRR pathfinder atmospheres-extended (PATMOS-x), version 5.3*. NOAA National Centers for environmental information: NOAA CDR Program.

Huang, K., Yi, C., Wu, D., Zhou, T., Zhao, X., Blanford, W. J., Wei, S., Wu, H., Ling, D., & Li, Z. (2015). Tipping point of a conifer forest ecosystem under severe drought. *Environmental Research Letters*, *10*(2), 24011. https://doi.org/10.1088/1748-9326/10/2/024011

Hulley, G. C., Hook, S. J., Abbott, E., Malakar, N., Islam, T., & Abrams, M. (2015). The ASTER global emissivity dataset (ASTER GED): Mapping Earth's emissivity at 100 meter spatial scale. *Geophysical Research Letters*, *42*(19), 7966–7976. https://doi.org/10.1002/2015gl065564

Jim, C. Y., & Peng, L. L. H. (2012). Weather effect on thermal and energy performance of an extensive tropical green roof. *Urban Forestry & Urban Greening*, *11*(1), 73–85. https://doi.org/10.1016/j.ufug.2011.10.001

Jimenez-Munoz, J. C., Sobrino, J. A., Skokovic, D., Mattar, C., & Cristobal, J. (2014). Land surface temperature retrieval methods from Landsat-8 thermal infrared sensor data. *IEEE Geoscience and Remote Sensing Letters*, *11*(10), 1840–1843. https://doi.org/10.1109/lgrs.2014.2312032

Konarska, J., Uddling, J., Holmer, B., Lutz, M., Lindberg, F., Pleijel, H., & Thorsson, S. (2016). Transpiration of urban trees and its cooling effect in a high latitude city. *International Journal of Biometeorology*, *60*(1), 159–172. https://doi.org/10.1007/s00484-015-1014-x

Li, X., Fan, W., Wang, L., Luo, M., Yao, R., Wang, S., & Wang, L. (2021). Effect of urban expansion on atmospheric humidity in Beijing-Tianjin-Hebei urban agglomeration. *Science of the Total Environment*, *759*, 144305. https://doi.org/10.1016/j.scitotenv.2020.144305

Li, X., Gong, P., Zhou, Y., Wang, J., Bai, Y., Chen, B., Hu, T., Xiao, Y., Xu, B., Yang, J., Liu, X., Cai, W., Huang, H., Wu, T., Wang, X., Lin, P., Li, X., Chen, J., He, C., … Zhu, Z. (2020). Mapping global urban boundaries from the global artificial impervious area (GAIA) data. *Environmental Research Letters*, *15*(9), 94044. https://doi.org/10.1088/1748-9326/ab9be3

Liu, X., Huang, Y., Xu, X., Li, X., Li, X., Ciais, P., Lin, P., Gong, K., Ziegler, A. D., Chen, A., Gong, P., Chen, J., Hu, G., Chen, Y., Wang, S., Wu, Q., Huang, K., Estes, L., & Zeng, Z. (2020). High-spatiotemporal-resolution mapping of global urban change from 1985 to 2015. *Nature Sustainability*, *3*(7), 564–570. https://doi.org/10.1038/s41893-020-0521-x

Lu, Y., Wu, P., Ma, X., Yang, H., & Wu, Y. (2020). Monitoring seasonal and diurnal surface urban Heat Islands variations using Landsat-scale data in Hefei, China, 2000–2017. *IEEE Journal of Selected Topics in Applied Earth Observations and Remote Sensing*, *13*, 6410–6423. https://doi.org/10.1109/jstars.2020.3035040

Luis, V. C., Jiménez, M. S., Morales, D., Kucera, J., & Wieser, G. (2005). Canopy transpiration of a Canary Islands pine forest. *Agricultural and Forest Meteorology*, *135*(1–4), 117–123. https://doi.org/10.1016/j.agrformet.2005.11.009

Malakar, N. K., Hulley, G. C., Hook, S. J., Laraby, K., Cook, M., & Schott, J. R. (2018). An operational land surface temperature product for Landsat thermal data: Methodology and validation. *IEEE Transactions on Geoscience and Remote Sensing*, *56*(10), 5717–5735. https://doi.org/10.1109/tgrs.2018.2824828

Manoli, G., Fatichi, S., Schläpfer, M., Yu, K., Crowther, T. W., Meili, N., Burlando, P., Katul, G. G., & Bou-Zeid, E. (2020). Reply to Martilli et al. (2020): Summer average urban-rural surface temperature differences do not indicate the need for urban heat reduction. https://osf.io/mwpna/

Mayor of London. (2018). *London environment strategy*. https://www.london.gov.uk/what-we-do/environment/london-environment-strategy

McDowell, N. G., & Allen, C. D. (2015). Darcy's law predicts widespread forest mortality under climate warming. *Nature Climate Change*, *5*(7), 669–672. https://doi.org/10.1038/nclimate2641

McPherson, E. G., Simpson, J. R., Xiao, Q., & Wu, C. (2011). Million trees Los Angeles canopy cover and benefit assessment. *Landscape and Urban Planning*, *99*(1), 40–50. https://doi.org/10.1016/j.landurbplan.2010.08.011

Meili, N., Manoli, G., Burlando, P., Bou-Zeid, E., Chow, W. T. L., Coutts, A. M., Daly, E., Nice, K. A., Roth, M., Tapper, N. J., Velasco, E., Vivoni, E. R., & Fatichi, S. (2020). An urban ecohydrological model to quantify the effect of vegetation on urban climate and hydrology (UT&C v1.0). *Geoscientific Model Development*, *13*(1), 335–362. https://doi.org/10.5194/gmd-13-335-2020

Meili, N., Manoli, G., Burlando, P., Carmeliet, J., Chow, W. T. L., Coutts, A. M., Roth, M., Velasco, E., Vivoni, E. R., & Fatichi, S. (2021). Tree effects on urban microclimate: Diurnal, seasonal, and climatic temperature differences explained by separating radiation, evapotranspiration, and roughness effects. *Urban Forestry & Urban Greening*, *58*, 126970. https://doi.org/10.1016/j.ufug.2020.126970

Meili, N., Paschalis, A., Manoli, G., & Fatichi, S. (2022). Diurnal and seasonal patterns of global urban dry islands. *Environmental Research Letters*, *17*(5), 054044. https://doi.org/10.1088/1748-9326/ac68f8

Miller, D. L., Alonzo, M., Meerdink, S. K., Allen, M. A., Tague, C. L., Roberts, D. A., & McFadden, J. P. (2022). Seasonal and interannual drought responses of vegetation in a California urbanized area measured using complementary remote sensing indices. *ISPRS Journal of Photogrammetry and Remote Sensing*, *183*, 178–195. https://doi.org/10.1016/j.isprsjprs.2021.11.002

Mora, C., Dousset, B., Caldwell, I. R., Powell, F. E., Geronimo, R. C., Bielecki, C. R., Counsell, C. W. W., Dietrich, B. S., Johnston, E. T., Louis, L. V., Lucas, M. P., McKenzie, M. M., Shea, A. G., Tseng, H., Giambelluca, T. W., Leon, L. R., Hawkins, E., & Trauernicht, C. (2017). Global risk of deadly heat. *Nature Climate Change*, *7*(7), 501–506. https://doi.org/10.1038/nclimate3322

Moskell, C., & Allred, S. B. (2013). Residents' beliefs about responsibility for the stewardship of park trees and street trees in New York City. *Landscape and Urban Planning*, *120*, 85–95. https://doi.org/10.1016/j.landurbplan.2013.08.002

Muñoz-Sabater, J., Dutra, E., Agustí-Panareda, A., Albergel, C., Arduini, G., Balsamo, G., Boussetta, S., Choulga, M., Harrigan, S., Hersbach, H., Martens, B., Miralles, D. G., Piles, M., Rodríguez-Fernández, N. J., Zsoter, E., Buontempo, C., & Thépaut, J.-N. (2021). ERA5-land: A state-of-the-art global reanalysis dataset for land applications. *Earth System Science Data*, *13*(9), 4349–4383. https://doi.org/10.5194/essd-13-4349-2021

Myint, S. W., Zheng, B., Talen, E., Fan, C., Kaplan, S., Middel, A., Smith, M., Huang, H. P., & Brazel, A. (2015). Does the spatial arrangement of urban landscape matter? Examples of urban warming and cooling in phoenix and Las Vegas. *Ecosystem Health and Sustainability*, *1*(4), 1–15. https://doi.org/10.1890/ehs14-0028.1

Nilon, C. H., Aronson, M. F. J., Cilliers, S. S., Dobbs, C., Frazee, L. J., Goddard, M. A., O'Neill, K. M., Roberts, D., Stander, E. K., Werner, P., Winter, M., & Yocom, K. P. (2017). Planning for the future of urban biodiversity: A global review of City-scale initiatives. *Bioscience*, *67*(4), 332–342. https://doi.org/10.1093/biosci/bix012

Nowak, D. J., & Greenfield, E. J. (2010). Evaluating the national land cover database tree canopy and impervious cover estimates across the conterminous United States: A comparison with photo-interpreted estimates. *Environmental Management*, *46*(3), 378–390. https://doi.org/10.1007/s00267-010-9536-9

Oke, T. R., & Cleugh, H. A. (1987). Urban heat storage derived as energy balance residuals. *Boundary-Layer Meteorology*, *39*(3), 233–245. https://doi.org/10.1007/bf00116120

Ouyang, W., Morakinyo, T. E., Ren, C., & Ng, E. (2020). The cooling efficiency of variable greenery coverage ratios in different urban densities: A study in a subtropical climate. *Building and Environment*, *174*, 106772. https://doi.org/10.1016/j.buildenv.2020.106772

Pares-Franzi, M., Sauri-Pujol, D., & Domene, E. (2006). Evaluating the environmental performance of urban parks in Mediterranean cities: An example from the Barcelona metropolitan region. *Environmental Management*, *38*(5), 750–759. https://doi.org/10.1007/s00267-005-0197-z

Paschalis, A., Chakraborty, T. C., Fatichi, S., Meili, N., & Manoli, G. (2021). Urban forests as main regulator of the evaporative cooling effect in cities. *AGU Advances*, *2*(2), e2020AV000303. https://doi.org/10.1029/2020av000303

Patz, J. A., Campbell-Lendrum, D., Holloway, T., & Foley, J. A. (2005). Impact of regional climate change on human health. *Nature*, *438*(7066), 310–317. https://doi.org/10.1038/nature04188

Peng, C., Ma, Z., Lei, X., Zhu, Q., Chen, H., Wang, W., Liu, S., Li, W., Fang, X., & Zhou, X. (2011). A drought-induced pervasive increase in tree mortality across Canada's boreal forests. *Nature Climate Change*, *1*(9), 467–471. https://doi.org/10.1038/nclimate1293

Perkins-Kirkpatrick, S. E., & Lewis, S. C. (2020). Increasing trends in regional heatwaves. *Nature Communications*, *11*(1), 3357. https://doi.org/10.1038/s41467-020-16970-7

Pfeifroth, U., Sanchez-Lorenzo, A., Manara, V., Trentmann, J., & Hollmann, R. (2018). Trends and variability of surface solar radiation in Europe based on surface- and satellite-based data records. *Journal of Geophysical Research: Atmospheres*, *123*(3), 1735–1754. https://doi.org/10.1002/2017jd027418

Pincetl, S., Gillespie, T., Pataki, D. E., Saatchi, S., & Saphores, J.-D. (2012). Urban tree planting programs, function or fashion? Los Angeles and urban tree planting campaigns. *GeoJournal*, *78*(3), 475–493. https://doi.org/10.1007/s10708-012-9446-x

Pourpeikari Heris, M., Bagstad, K. J., Troy, A. R., & O'Neil-Dunne, J. P. M. (2022). Assessing the accuracy and potential for improvement of the National Land Cover Database's tree canopy cover dataset in urban areas of the conterminous United States. *Remote Sensing*, *14*(5), 1219 https://www.mdpi.com/2072-4292/14/5/1219

Rahman, M. A., Hartmann, C., Moser-Reischl, A., von Strachwitz, M. F., Paeth, H., Pretzsch, H., Pauleit, S., & Rötzer, T. (2020). Tree cooling effects and human thermal comfort under contrasting species and sites. *Agricultural and Forest Meteorology*, *287*, 107947. https://doi.org/10.1016/j.agrformet.2020.107947

Rahman, M. A., Stratopoulos, L. M. F., Moser-Reischl, A., Zölch, T., Häberle, K.-H., Rötzer, T., Pretzsch, H., & Pauleit, S. (2020). Traits of trees for cooling urban heat islands: A meta-analysis. *Building and Environment*, *170*, 106606. https://doi.org/10.1016/j.buildenv.2019.106606

Rana, G., De Lorenzi, F., Mazza, G., Martinelli, N., Muschitiello, C., & Ferrara, R. M. (2020). Tree transpiration in a multi-species Mediterranean garden. *Agricultural and Forest Meteorology*, *280*, 107767. https://doi.org/10.1016/j.agrformet.2019.107767

Schwaab, J., Meier, R., Mussetti, G., Seneviratne, S., Burgi, C., & Davin, E. L. (2021). The role of urban trees in reducing land surface temperatures in European cities. *Nature Communications*, *12*(1), 6763. https://doi.org/10.1038/s41467-021-26768-w

Sexton, J. O., Song, X.-P., Feng, M., Noojipady, P., Anand, A., Huang, C., Kim, D.-H., Collins, K. M., Channan, S., DiMiceli, C., & Townshend, J. R. (2013). Global, 30-m resolution continuous fields of tree cover: Landsat-based rescaling of MODIS vegetation continuous fields with lidar-based estimates of error. *International Journal of Digital Earth*, *6*(5), 427–448. https://doi.org/10.1080/17538947.2013.786146

Speak, A., Montagnani, L., Wellstein, C., & Zerbe, S. (2020). The influence of tree traits on urban ground surface shade cooling. *Landscape and Urban Planning*, *197*, 103748. https://doi.org/10.1016/j.landurbplan.2020.103748

Wang, C., Wang, Z.-H., Wang, C., & Myint, S. W. (2019). Environmental cooling provided by urban trees under extreme heat and cold waves in U.S. cities. *Remote Sensing of Environment*, *227*, 28–43. https://doi.org/10.1016/j.rse.2019.03.024

Wang, H., Ouyang, Z., Chen, W., Wang, X., Zheng, H., & Ren, Y. (2011). Water, heat, and airborne pollutants effects on transpiration of urban trees. *Environmental Pollution*, *159*(8–9), 2127–2137. https://doi.org/10.1016/j.envpol.2011.02.031

Wang, J., Zhou, W., & Jiao, M. (2022). Location matters: Planting urban trees in the right places improves cooling. *Frontiers in Ecology and the Environment*, *20*(3), 147–151. https://doi.org/10.1002/fee.2455

Wang, J., Zhou, W., Jiao, M., Zheng, Z., Ren, T., & Zhang, Q. (2020). Significant effects of ecological context on urban trees' cooling efficiency. *ISPRS Journal of Photogrammetry and Remote Sensing*, *159*, 78–89. https://doi.org/10.1016/j.isprsjprs.2019.11.001

Xian, G., Shi, H., Zhou, Q., Auch, R., Gallo, K., Wu, Z., & Kolian, M. (2022). Monitoring and characterizing multi-decadal variations of urban thermal condition using time-series thermal remote sensing and dynamic land cover data. *Remote Sensing of Environment*, *269*, 112803. https://doi.org/10.1016/j.rse.2021.112803

Yang, Q., Huang, X., Tong, X., Xiao, C., Yang, J., Liu, Y., & Cao, Y. (2022). Global assessment of urban trees' cooling efficiency based on satellite observations. *Environmental Research Letters*, *17*(3), 34029. https://doi.org/10.1088/1748-9326/ac4c1c

Yao, N., Konijnendijk van den Bosch, C. C., Yang, J., Devisscher, T., Wirtz, Z., Jia, L., Duan, J., & Ma, L. (2019). Beijing's 50 million new urban trees: Strategic governance for large-scale urban afforestation. *Urban Forestry & Urban Greening*, *44*, 126392. https://doi.org/10.1016/j.ufug.2019.126392

Young, R. F. (2011). Planting the living City. *Journal of the American Planning Association*, *77*(4), 368–381. https://doi.org/10.1080/01944363.2011.616996

Yu, Z., Xu, S., Zhang, Y., Jorgensen, G., & Vejre, H. (2018). Strong contributions of local background climate to the cooling effect of urban green vegetation. *Scientific Reports*, *8*(1), 6798. https://doi.org/10.1038/s41598-018-25296-w

Zeppel, M. J. B., Macinnis-Ng, C. M. O., Yunusa, I. A. M., Whitley, R. J., & Eamus, D. (2008). Long term trends of stand transpiration in a remnant forest during wet and dry years. *Journal of Hydrology*, *349*(1–2), 200–213. https://doi.org/10.1016/j.jhydrol.2007.11.001

Zhao, J., Meili, N., Zhao, X., & Fatichi, S. (2023). Urban vegetation cooling potential during heatwaves depends on background climate. *Environmental Research Letters*, *18*(1), 14035. https://doi.org/10.1088/1748-9326/acaf0f

Zhao, J., Zhao, X., Liang, S., Wang, H., Liu, N., Liu, P., & Wu, D. (2021). Dynamic cooling effects of permanent urban green spaces in Beijing, China. *Remote Sensing*, *13*(16), 3282 https://www.mdpi.com/2072-4292/13/16/3282

Zhao, J., Zhao, X., Liang, S., Zhou, T., Du, X., Xu, P., & Wu, D. (2020). Assessing the thermal contributions of urban land cover types. *Landscape and Urban Planning*, *204*, 103927. https://doi.org/10.1016/j.landurbplan.2020.103927

Zhao, L., Oppenheimer, M., Zhu, Q., Baldwin, J. W., Ebi, K. L., Bou-Zeid, E., Guan, K., & Liu, X. (2018). Interactions between urban heat islands and heat waves. *Environmental Research Letters*, *13*(3), 34003. https://doi.org/10.1088/1748-9326/aa9f73

Zheng, S., Guldmann, J.-M., Wang, Z., Qiu, Z., He, C., & Wang, K. (2021). Experimental and theoretical study of urban tree instantaneous and hourly transpiration rates and their cooling effect in hot and humid area. *Sustainable Cities and Society*, *68*, 102808. https://doi.org/10.1016/j.scs.2021.102808

Zhou, W., Huang, G., Pickett, S. T. A., Wang, J., Cadenasso, M. L., McPhearson, T., Grove, J. M., & Wang, J. (2021). Urban tree canopy has greater cooling effects in socially vulnerable communities in the US. *One Earth*, *4*(12), 1764–1775. https://doi.org/10.1016/j.oneear.2021.11.010

Zhou, W., Wang, J., & Cadenasso, M. L. (2017). Effects of the spatial configuration of trees on urban heat mitigation: A comparative study. *Remote Sensing of Environment*, *195*, 1–12. https://doi.org/10.1016/j.rse.2017.03.043

Zhu, Z., Piao, S., Myneni, R. B., Huang, M., Zeng, Z., Canadell, J. G., Ciais, P., Sitch, S., Friedlingstein, P., Arneth, A., Cao, C., Cheng, L., Kato, E., Koven, C., Li, Y., Lian, X., Liu, Y., Liu, R., Mao, J., … Zeng, N. (2016). Greening of the earth and its drivers. *Nature Climate Change*, *6*(8), 791–795. https://doi.org/10.1038/nclimate3004

SUPPORTING INFORMATION

Additional supporting information can be found online in the Supporting Information section at the end of this article.

How to cite this article: Zhao, J., Zhao, X., Wu, D., Meili, N., & Fatichi, S. (2023). Satellite-based evidence highlights a considerable increase of urban tree cooling benefits from 2000 to 2015. *Global Change Biology*, *00*, 1–13. https://doi.org/10.1111/gcb.16667